07.2;07.3

Analysis of the internal optical losses of the 89X nm-range intracavity-contacted vertical-cavity surface-emitting lasers

© S.A. Blokhin[1], M.A. Bobrov[1], A.A. Blokhin[1], J.N. Kovach[1], N.A. Maleev[1], A.G. Kuzmenkov[1], Yu.M. Zadiranov[1], M.M. Kulagina[1], Yu.A. Guseva[1], A.P. Vasyliev[2], V.M. Ustinov[2]

[1] Ioffe Institute, St. Petersburg, Russia
[2] Submicron Heterostructures for Microelectronics, Research & Engineering Center, RAS, St. Petersburg, Russia
E-mail: blokh@mail.ioffe.ru

Received August 31, 2023
Revised September 11, 2023
Accepted September 12, 2023

The paper presents a study of static characteristics of the 89X nm-range vertical-cavity surface-emitting lasers in the geometry of a vertical-microcavity with intracavity contacts and diamond-shaped oxide-confined current aperture. The proposed microcavity design could simultaneously provide a single-mode lasing regime and narrow laser-emission line. The internal optical losses were evaluated for devices with different-size oxide-confined current apertures. It was shown that the proposed design could provide a current injection efficiency of more than $\sim 80\%$ and internal optical loss less than $12\,\mathrm{cm}^{-1}$ (for the effective cavity length of $3.4\,\mu$m) in the current aperture size range of $1.5-3\,\mu$m, which is extremely important for minimizing threshold currents in single-mode lasers with small apertures.

Keywords: vertical-cavity surface-emitting laser, single-mode lasing, polarization, linewidth, modulation bandwidth.

DOI: 10.61011/TPL.2023.10.57066.19717

In the latest years, an increasing attention is being paid to the issue of minimizing the overall dimensions and energy consumption of various-type atomic sensors, which is possible only if injection laser diodes are used instead of gas-discharge lamps for optical pumping of alkali-metal atoms and optical detection of their states [1]. However, laser sources for compact atomic sensors are to satisfy simultaneously a number of specific requirements: exact correspondence of the laser emission frequency to a specific energy transition in the energy structure of the used alkali atom (isotopes ^{133}Cs, ^{85}Ru or ^{87}Ru), single-mode lasing and narrow spectral line, linearly polarized emission with a fixed direction of the polarization plane, possibility of reliable operation at high operating temperatures, fast response, and low power consumption. External-cavity lasers widely used in spectroscopy are suitable only for demonstrating the effect or for testing one or another concept for creating atomic sensors, while the distributed-feedback lasers can hardly be precisely tuned to the required wavelength.

A unique opportunity is offered by vertical-cavity surface-emitting lasers (VCSELs); such a laser is a vertical microcavity constrained by two distributed Bragg reflectors (DBRs). Lasers of this type are characterized by the possibility of realizing single-mode lasing, sub-milliampere threshold currents, high temperature stability, and high spatial symmetry of the output optical emission [2]. Moreover, in this case it becomes possible to compactly arrange the laser emitter and optical scheme for focusing the emission directly to the vicinity of the gas cell. At present, VCSELs of the 7XX and 8XX nm spectral ranges have been successfully tested in quantum magnetometers [3], nuclear magnetic gyroscopes [4], and quantum frequency standards [5]. The most straightforward approach to realizing the single-mode lasing is based on reducing the area of charge carrier injection into the active region with the aid of a current aperture [6]; at the same time, to narrow the laser emission line, it is necessary to increase the cavity photon lifetime by increasing the optical cavity width. However, in the case of the VCSEL design implying carrier injection through doped DBRs, this entails an increase in the series resistance and a risk of enhancements of internal optical losses, which negatively affects the long-term reliability of single-mode lasers (a sharp growth of current density).

Recently we have proposed and successfully tested an original 8XX nm VCSEL design implying carrier injection through intracavity contacts (IC); this model allows simultaneous reduction in the series resistance and emission linewidth [7]. This paper presents the results of analyzing the internal optical losses and current injection efficiency in single-mode lasers of such a design.

The IC-VCSEL under study is designed as a hybrid vertical optical microcavity constrained between the lower semiconductor DBR $Al_{0.15}Ga_{0.85}As/Al_{0.9}Ga_{0.1}As$ and upper dielectric DBR SiO_2/Ta_2O_5. The number of pairs in DBR is chosen so as to realize the scheme of light extraction through the upper DBR. Figure 1 demonstrates the distribution of the standing wave electromagnetic field, as well as profiles of the refractive index and doping of the heterostructure layers, in the longitudinal direction (in the direction of epitaxial growth of the

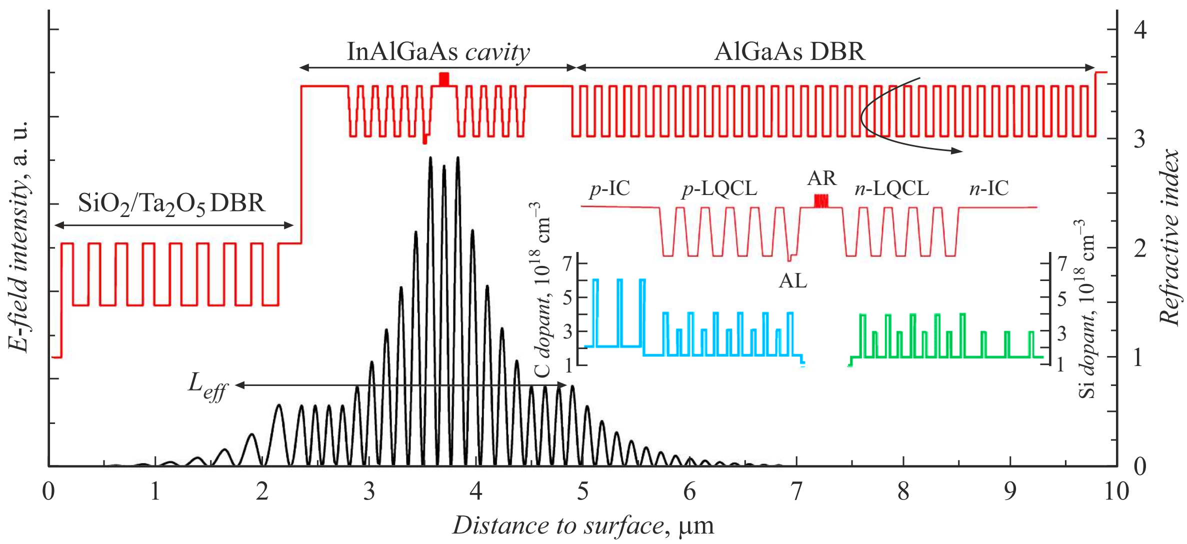

Figure 1. Longitudinal distribution of the standing wave electromagnetic field, refractive index and dopants (in the inset) in the IC-VCSEL microcavity. DBR — distributed Bragg reflector, IC — intracavity contact, LQCL — low-Q composite lattice, AR — active region, AL — aperture layer.

layers). The active region consists of five $In_{0.08}Ga_{0.92}As$ quantum wells separated by barrier layers $Al_{0.15}Ga_{0.85}As$. Charge carriers are injected into the active region through IC layers $Al_{0.15}Ga_{0.85}As$ and low-Q composite lattices (LQCL) $Al_{0.15}Ga_{0.85}As/Al_{0.9}Ga_{0.1}As$. To reduce potential barriers at the $Al_{0.15}Ga_{0.85}As/Al_{0.9}Ga_{0.1}As$ heterointerfaces, gradient interfaces with a higher doping level, namely, 2–3 times higher than the average doping level in the cavity layers ($\sim 2 \cdot 10^{18}\,cm^{-3}$), have been created. Using asymmetric pairs of layers p-$Al_{0.15}Ga_{0.85}As/Al_{0.9}Ga_{0.1}As$ and n-$Al_{0.15}Ga_{0.85}As/Al_{0.9}Ga_{0.1}As$ in LQCL, we succeeded in efficiently redistributing the longitudinal mode electromagnetic field and increasing the effective length of the L_{eff} cavity by more than 2 times compared to that in the classical VCSEL design with carrier injection through the doped DBRs. To reduce the absorption on free carriers (especially in the p-type layers), a modulated profile of doping the IC layers with impurities was used, when heavily doped regions are located in local minima of the wave electromagnetic field. To ensure simultaneously the current and optical confinement, an $AlAs/Al_{0.9}Ga_{0.1}As$ aperture layer was introduced into the IC-VCSEL heterostructure, which allows formation of the current aperture by selective water-vapor oxidation of AlGaAs layers at the stage of manufacturing the IC-VCSEL crystals. In addition, the aperture layer was also set in the field minimum in order to decay the effect of light scattering/diffraction at the oxide–semiconductor interface taking place when the size of the oxide-confined aperture is reduced [8]. A more detailed description of the device design and specific features of the IC-VCSEL manufacturing process are given in [7,9].

Figure 2, a shows the dependences of the slope efficiency (the optical power rise rate of a laser with the current above the lasing threshold) on the characteristic size of the oxide-confined current aperture of IC-VCSEL with eight SiO_2/Ta_2O_5 pairs in the upper DBR; the dependences were measured at room temperature in the continuous operation mode. To minimize the influence of thermal effects, the slope efficiency was evaluated in the vicinity of the lasing threshold. When the current aperture size is less than $3\,\mu$m, a decrease in the slope efficiency is observed. This fact is not associated with variations in the laser mode composition, since low-current lasing proceeds through the fundamental mode (the single-mode lasing is maintained over the entire range of currents when the apertures are smaller than $2.5\,\mu$m). Moreover, as the current aperture size decreases, a sharp increase in the threshold current density is observed (Fig. 2, a).

As is known, the VCSEL slope efficiency η_{SE} depends on mirror losses α_m, internal optical losses α_{int}, and current injection efficiency η_{int}:

$$\eta_{SE} = F_T \eta_{int} \left(\frac{E_{ph}}{q}\right)\left(\frac{\alpha_m}{\alpha_m + \alpha_{int}}\right),$$

where q is the elementary charge, E_{ph} is the photon energy. In the case of using mirrors with different reflection coefficients, it is necessary to introduce normalization factor F_T in order to account for the share of optical power extracted through the upper mirror [2]. Hence, we can assume the occurrence of both a decrease in efficiency η_{int} due to activation of additional mechanisms for charge carrier leakage and emergence of additional internal optical losses. To clarify this point, there was analyzed the effect of the level of mirror losses (variations due to changes in the number of pairs in dielectric DBR) on slope efficiency of lasers with different-size oxide-confined current apertures similarly to [10–12]. The effect of the charge carriers concentrating along the current aperture perimeter, which

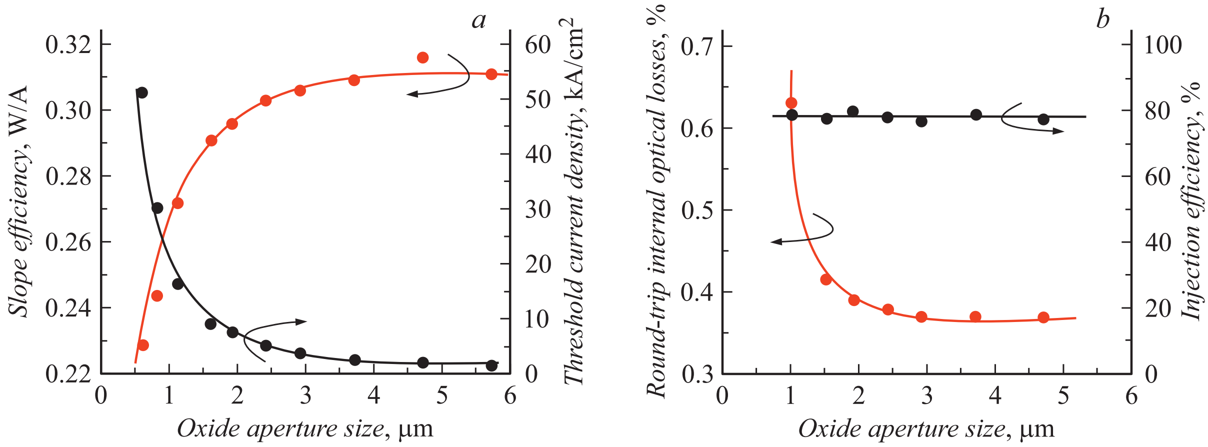

Figure 2. *a* — slope efficiency and threshold current density versus the oxide-confined aperture size for IC-VCSEL with an upper DBR based on eight SiO_2/Ta_2O_5 pairs; *b* — internal optical losses due to passing through the IC-VCSEL cavity versus the oxide-confined aperture size. The temperature is 20°C.

leads to nonuniformity of the carrier injection into the active region within the aperture area, manifests itself most intensely in wide-aperture devices with a characteristic aperture size of more than 6 μm; therefore, the current injection efficiency in the devices under study depends on the aperture size only slightly and amounts to 78–80% (Fig. 2, *b*). The situation is different in the case of losses α_{int}: with increasing aperture size, loss α_{int} decreases drastically and gets fixed at $\sim$ 0.37% of that due to passing through the cavity at the aperture size exceeding 2.5 μm (Fig. 2, *b*) which matches the distributed mirror losses of less than 11 cm^{-1} (at the effective cavity length of 3.4 μm). Thus, the slope efficiency reduction at small aperture sizes is associated mainly with an increase in internal optical losses due to light scattering/diffraction from the oxide–semiconductor interface [8,10]. The attained levels of internal optical losses are inferior to the record-low losses in the 98X nm monolithic VCSEL with a 12 μm current aperture [11] and 98X nm monolithic IC-VCSEL with a current aperture of 10 ,μm [12]. However, they correlate well with data for a 85X nm monolithic short-cavity VCSEL in a wide range of aperture sizes [10], which indicates the efficiency of the proposed approach to creating 89X nm VCSELs for compact atomic sensors.

Thus, the paper presents the results of analyzing the level of internal optical losses in 89X nm VCSELs with intracavity contacts and diamond-shaped oxide-confined current aperture. It is shown that the proposed laser design provides a current injection efficiency of more than $\sim$ 80% at internal optical losses below 12 cm^{-1}, which is extremely important for minimizing threshold currents in single-mode lasers with small aperture sizes.

Financial support

The study was partially supported by the RF Ministry of Science and Higher Education (project FFUG-2022-0011).

Conflict of interests

The authors declare that they have no conflict of interests.

References

[1] J. Kitching, Appl. Phys. Rev., **5** (3), 031302 (2018). DOI: 10.1063/1.5026238.
[2] R. Michalzik, *VCSELs: fundamentals, technology and applications of vertical-cavity surface-emitting lasers* (Springer-Verlag, Berlin, 2013).
DOI: 10.1007/978-3-642-24986-0
[3] P.D.D. Schwindt, B. Lindseth, S. Knappe, V. Shah, J. Kitching, L.-A. Liew, Appl. Phys. Lett., **90** (8), 081102 (2007). DOI: 10.1063/1.2709532
[4] D. Meyer, M. Larsen, Gyroscopy Navig., **5** (2), 75 (2014). DOI: 10.1134/S2075108714020060
[5] S. Knappe, V. Shah, P.D.D. Schwindt, L. Hollberg, J. Kitching, L.-A. Liew, J. Moreland, Appl. Phys. Lett., **85** (9), 1460 (2004). DOI: 10.1063/1.1787942
[6] W. Nakwaski, Opto-Electron. Rev., **19** (1), 119 (2011). DOI: 10.2478/s11772-010-0075-y
[7] S.A. Blokhin, N.A. Maleev, M.A. Bobrov, A.G. Kuzmenkov, A.P. Vasiliev, Yu.M. Zadiranov, M.M. Kulagina, A.A. Blokhin, Yu.A. Guseva, A.M. Ospennikov, M.V. Petrenko, A.G. Gladyshev, A.Yu. Egorov, I.I. Novikov, L.Ya. Karachinsky, D.V. Denisov, V.M. Ustinov, Quantum Electron., **49** (2), 187 (2019). DOI: 10.1070/QEL16871.
[8] E.R. Hegblom, D.I. Babic, B.J. Thibeault, L.A. Coldren, IEEE J. Sel. Top. Quantum Electron., **3** (2), 379 (1997). DOI: 10.1109/2944.605682
[9] N.A. Maleev, A.G. Kuzmenkov, M.M. Kulagina, Yu.M. Zadiranov, A.P. Vasiliev, S.A. Blokhin, A.S. Shulenkov, S.I. Troshkov, A.G. Gladyshev, A.M. Nadtochiy, M.M. Pavlov, M.A. Bobrov, D.E. Nazaruk, V.M. Ustinov, Semiconductors, **47** (7), 993 (2013). DOI: 10.1134/s1063782613070166.
[10] M. Jungo, F.M. di Sopra, D. Erni, W. Baechtold, J. Appl. Phys., **91** (9), 5550 (2002). DOI: 10.1063/1.1462422

[11] S.A. Blokhin, N.A. Maleev, A.G. Kuzmenkov, A.V. Sakharov, M.M. Kulagina, Y.M. Shernyakov, I.I. Novikov, M.V. Maximov, V.M. Ustinov, A.R. Kovsh, S.S. Mikhrin, N.N. Ledentsov, G. Lin, J.Y. Chi, IEEE J. Quantum Electron., **42** (9), 851 (2006). DOI: 10.1109/JQE.2006.880125
[12] G.M. Yang, M.H. MacDugal, V. Pudikov, P.D. Dapkus, IEEE Photon. Technol. Lett., **7** (11), 1228 (1995). DOI: 10.1109/68.473454

Translated by Solonitsyna Anna